

Self-Assembly of a Liquid Crystalline Anisotropic Gel

Li Guan and Yue Zhao*

Département de chimie, Université de Sherbrooke, Sherbrooke, Québec, Canada J1K 2R1, and Centre de recherche en science et ingénierie des macromolécules (CERSIM), Université Laval, Québec, Canada G1K 7P4

Received July 13, 2000. Revised Manuscript Received September 20, 2000

A new azobenzene-containing gelator for low-molar-mass liquid crystals (LCs) was synthesized. It can effectively gel nematic LCs such as E7 through the formation of a hydrogen-bonded network. Moreover, an intriguing self-assembly process was observed. When thin films of the E7/gelator mixture, cast on CaF₂ crystal windows or glass slides, are cooled from the isotropic phase, at temperatures below but close to the sol–gel phase transition, aggregation of the gelator starts from the edge of the film, and the fiberlike aggregates grow predominantly normal to the edge, leading to the formation of an oriented network at the macroscopic scale in the liquid gel state. On further cooling through the phase transition from liquid gel to nematic gel, the aligned fiberlike aggregates induce a long-range molecular orientation of E7, in the direction perpendicular to the fibers. The end result of this is a self-assembled anisotropic LC gel formed in the absence of any external effects such as surface treatment for the substrates or irradiation for the azobenzene groups on the gelator molecules.

Introduction

Liquid crystalline anisotropic gels refer to oriented low-molar-mass liquid crystals (LCs) stabilized by a polymer network. Generally, the long-range LC orientation in these materials is achieved either by surface effect or electric field, prior to the polymerization of a reactive monomer dissolved in the LC. Subsequent polymerization inside an oriented LC environment results in an oriented polymer network, which is microphase-separated from the LC and able to retain permanently the LC orientation or textures in the LC phases.^{1,2} The LC orientation can be altered by external stimuli such as electric field and change in temperature, but the initial orientational state is recovered once the external stimuli are removed. Such a memory effect makes LC anisotropic gels attractive for many potential applications.^{3,4} Recent studies in our laboratory explored a new LC orientation mechanism to make anisotropic gels.^{5–7} The approach uses the well-known optical alignment of azobenzene when exposed to linearly polarized light, as a result of its photoisomerization.⁸ In essence, reactive diacrylate monomers carrying azobenzene groups were synthesized and dissolved in

nematic LCs to obtain anisotropic gels through optical alignment, in the absence of surface orientation layers (rubbed surfaces) or electric field. It was demonstrated that when mixed with a LC compound, the azobenzene monomer could first induce a long-range LC orientation through its own alignment under irradiation and then lock in the LC orientation through its anisotropic network formed upon polymerization.^{5–7} As the LC orientation is dictated by the orientation of the azobenzene monomer, the method offers new possibilities for spatially modulating or configuring the LC orientation that the surface alignment cannot do. Studies are underway applying this approach to various LCs.

In the systems studied previously,^{5–7} the azobenzene networks formed by polymerizations of the diacrylate monomers are covalent. It would be of interest to explore the use of noncovalent networks bearing azobenzene groups in the preparation of LC anisotropic gels that possess new properties. For instance, a combination of the dynamic nature of hydrogen-bonded networks with the optical alignment of azobenzene may lead to a system whose network structure has a reduced effect on the LC phase transition temperatures and can be thermally redissociated or altered by external stimuli more easily than covalent networks. As a matter of fact, on the basis of the numerous studies on the gelation of organic solvents,^{9,10} Kato and co-workers have recently showed that LCs can be gelled by the formation of hydrogen-bonded molecular aggregates.^{11–13} The gelators are generally amino acid or amide derivatives. In

* Address all correspondence to this author at the Université de Sherbrooke.

(1) Hikmet, R. A. M. In *Liquid Crystals in Complex Geometries Formed by Polymer and networks*; Crawford, G. P., Zumer, S., Eds.; Taylor & Francis: London, 1996; p 53.

(2) Yang, D.-K.; Chien, L.-C.; Fung, Y. K. In *Liquid Crystals in Complex Geometries Formed by Polymer and networks*; Crawford, G. P., Zumer, S., Eds.; Taylor & Francis: London, 1996; p 103.

(3) Hikmet, R. A. M. *J. Mater. Chem.* **1999**, *9*, 1921.

(4) Hikmet, R. A. M.; Kemperman, H. *Nature* **1998**, *392*, 476.

(5) Zhao, Y.; Chenard, Y.; Paiement, N. *Macromolecules* **2000**, *33*, 1094.

(6) Zhao, Y.; Chenard, Y. *Macromolecules* **2000**, *33*, 5891.

(7) Zhao, Y.; Chenard, Y.; Galstain, T. *Appl. Phys. Lett.*, in press.

(8) Natansohn, A.; Rochon, P.; Gosselin, J.; Xie, S. *Macromolecules* **1992**, *25*, 2268.

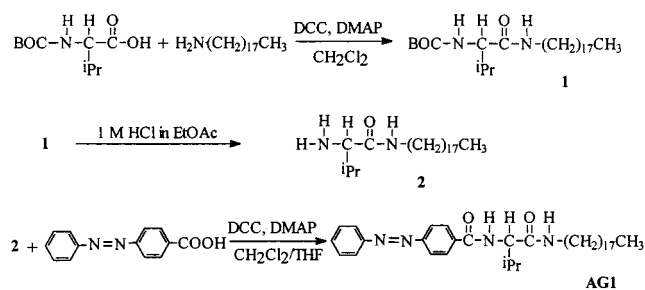
(9) Terech, P.; Weiss, R. G. *Chem. Rev.* **1997**, *97*, 3133.

(10) Geiger, C.; Stanescu, M.; Chen, L.; Whitten, D. G. *Langmuir* **1999**, *15*, 2241.

(11) Mizoshita, N.; Hanabusa, K.; Kato, T. *Adv. Mater.* **1999**, *5*, 392.

(12) Mizoshita, N.; Kutsuna, T.; Hanabusa, K.; Kato, T. *Chem. Commun.* **1999**, 701.

(13) Yabuuchi, K.; Rowan, A. E.; Nolte, R. J. M.; Kato, T. *Chem. Mater.* **2000**, *12*, 440.

Scheme 1. Synthesis of the Azobenzene Gelator

their studies, rubbed surfaces were used to promote the LC orientation, and anisotropic gels with H-bonded networks dispersed in nematic^{11,13} and smectic LCs¹² were obtained. In the case of nematic anisotropic gels, three thermoreversible phases were observed, namely, liquid, liquid gel, and LC gel. The liquid gel is characterized by randomly dispersed fibrous aggregates, i.e., an isotropic H-bonded network, surrounded by the LC compound in its isotropic phase; whereas in the LC gel state, in the presence of the isotropic network, the LC compound is in its nematic phase and has a long-range orientation induced by rubbed surfaces. For their smectic anisotropic gel,¹² as the sol-gel phase transition occurs within the smectic phase of the LC compound, the H-bonded aggregates were found to form between the smectic layers whose directors are aligned in the surface rubbing direction; consequently, an anisotropic H-bonded network is formed, with the aggregates aligned perpendicularly to the surface rubbing direction. All the reported gelators used to gel LCs contain no azobenzene groups.

In this paper, we report on the synthesis of a new gelator bearing azobenzene group, its gelling properties for a nematic LC, and, more interestingly, an intriguing self-assembly process developing in the absence of rubbed surfaces or irradiation that can be applied to the azobenzene-containing gelator. This process leads to macroscopically aligned fibrous aggregates, i.e., oriented H-bonded network, in the liquid gel and, in the LC gel, the induction of oriented LCs by the aligned fibrous aggregates.

Experimental Section

1. Synthesis of the Azobenzene Gelator. The synthetic route used to prepare the azobenzene gelator, AG1, is shown in Scheme 1. The hydrogen-bonding moieties of AG1 include an aromatic amide and an alkyl amide unit. All reagents were purchased either from Aldrich or Sigma and used without further purification. Dry solvents were freshly distilled under anhydrous conditions: methylene chloride (CH₂Cl₂) from calcium hydride; tetrahydrofuran (THF) from sodium-benzophenone. The reactions were monitored by thin-layer chromatography (TLC). Characterizations of the compounds were performed using proton nuclear magnetic resonance (Bruker AC-F 300), differential scanning calorimetry (Perkin-Elmer DSC7), mass spectroscopy (Micromass ZAB-1F), and infrared (Bomern MB-102 FTIR) and UV-vis spectroscopy (HP-8452A). More details on the synthesis and characterization results are outlined below.

Compound 1. A solution of *N*-*t*-BOC-L-valine (434 mg, 2 mmol), octadecylamine (540 mg, 2 mmol), and 4-(dimethylamino)pyridine (DMAP) (50 mg, 10%) in dry CH₂Cl₂ (20 mL) was stirred at 0 °C for 30 min; then *N,N*-dicyclohexylcarbodiimide (DCC) (453 mg, 2.2 mmol) was added in. The resulting mixture was stirred for another 30 min in an ice-water bath

before being warmed rapidly to room temperature and stirred overnight. Afterward, the precipitate was filtered out, and the solvent removed under reduced pressure. Finally, the products were separated by silica gel column chromatography (hexane/methanol) to have the compound 1 collected as a white solid (612 mg, 64%). Mp: 82 °C. ¹H NMR (δ/ppm) (DMSO-*d*₆): 7.77 (1H, t), 6.54 (1H, d), 4.10 (1H, q), 3.12~2.95 (2H, m), 1.87 (1H, m), 1.39 (9H, s), 1.25 (32H, br s), 0.8~0.78 (9H, m). IR (ν/cm⁻¹) (KBr): 1650 (C=O of amides), 1692 (m) (C=O of urethanes), 3316 (m) (N-H of urethanes and amides). MS (*m/e*): 468 (M⁺).

Compound 2. Compound 1 was dissolved in 1 M solution of HCl in ethyl acetate. The reaction mixture was stirred at room temperature until the disappearance of the starting materials as determined by TLC (after about 30 h). After evaporation of the solvent, colorless, oily compound 2 was obtained. The crude product was directly used for next reaction without further purification.

AG1. A solution of 4-phenylazobenzoic acid (250 mg, 1.10 mmol), crude compound 2 (270 mg, 0.73 mmol), and DMAP (9 mg, 0.07 mmol) was prepared in dry CH₂Cl₂ (10 mL) and THF (2 mL). After it was stirred at 0 °C for 30 min, DCC (286 mg, 1.39 mmol) was added in. The resulting mixture was stirred for another 30 min in an ice-water bath. The reaction mixture was warmed to room temperature slowly and stirred for over 24 h. The precipitate was filtered out, and the filtrate was dried under reduced pressure. AG1 (the gelator) was obtained after purification by column chromatography on silica gel (CH₂-Cl₂/THF), yielding a light yellow solid (234 mg, 56%). Mp: 201 °C. ¹H NMR (δ/ppm) (THF-*d*₈): 8.08 (2H, d), 7.96 (4H, d), 7.78 (1H, d), 7.55 (3H, m), 7.41 (1H, t), 4.37 (1H, t), 3.30~3.05 (2H, m), 2.25 (1H, m), 1.49 (2H, m), 1.30 (30H, brs), 0.97 (6H, d), 0.88 (3H, t). IR (ν/cm⁻¹) (KBr): 1629 (C=O of aromatic amide), 1657 (C=O of alkyl amide), 3285 (N-H of urethanes and amides). MS (*m/e*): 576 (M⁺). UV (λ/nm) (THF): 328 (π → π*, azobenzene).

2. Preparation of Anisotropic Gels. The nematic LC used is E7 purchased from EM Industries. It is a eutectic mixture mainly composed of cyanobiphenyl compounds and has a nematic-isotropic transition temperature *T*_{ni} of 58 °C. To prepare the gel, normally the LC and gelator can be heated into the isotropic phase to ensure the homogeneous mixing. In this study, as the AG1 has a high melting temperature (201 °C), to avoid thermal decomposition, the gelator and E7 were dissolved in a small amount of THF to get a homogeneous solution, and the gel was obtained after removing the solvent by first heating the mixture at 80 °C for a couple of hours and then at 40 °C in a vacuum oven for another 4 h. For all experiments, the E7/AG1 mixture was heated to the isotropic phase for at least 5 min before cooling to the liquid gel and LC gel states. Unless otherwise stated, thin films of about 8 μm thick were cast from warmed mixtures (~80 °C) either between two CaF₂ windows, which are transparent to UV and infrared, or microscope glass slides. An Instec hot stage was used to control and change the temperature of the mixtures.

3. Characterization of Anisotropic Gels. Optical micrographs were taken on a Leitz MP-polarizing microscope, and scanning electron microscopy (SEM) observations conducted on a JEOL JSC-840A system. The molecular order in self-assembled anisotropic gels, i.e., the orientation of both H-bonded network and E7, was characterized using infrared dichroism. Details about the measurement of the order parameter have already been reported.^{6,5-7} Polarized infrared spectra were recorded on a Bomem MB-200 FTIR spectrometer, equipped with a wire-grid polarizer and a DTGS detector. A homemade thermostat sample holder (±2 °C) was used for the variable-temperature infrared measurements.

Results and Discussion

AG1 was found to be able to gel E7. Figure 1 shows an example of the DSC heating and cooling curves that reveal the three thermoreversible phases. For the mixture containing 0.5 mol % of AG1, on cooling from the liquid phase at 10 °C/min, the sol-gel transition,

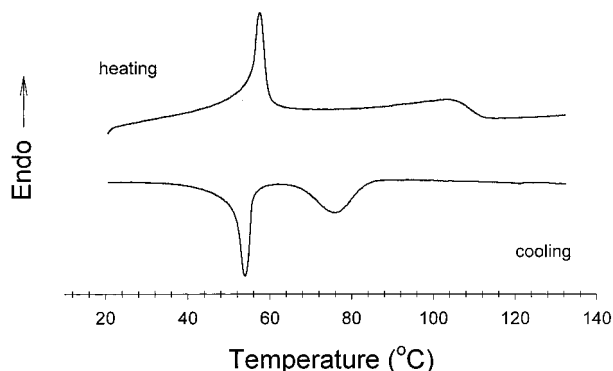


Figure 1. DSC heating and cooling curves (10 °C/min) for the mixture of E7/AG1 containing 0.5 mol % AG1.

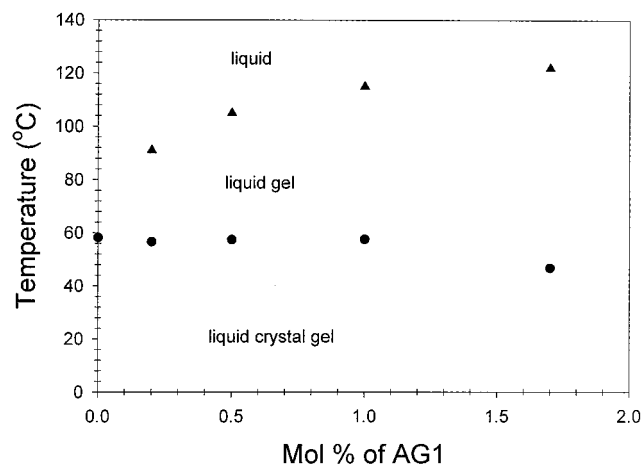


Figure 2. Phase diagram for the mixture of E7/AG1 on heating.

corresponding to the aggregation (or crystallization) of the gelator, is indicated by an exotherm around 75 °C. As expected for a crystallization process that generally displays an important supercooling, this exotherm is strongly dependent on the cooling rate, appearing at higher temperatures at slower cooling rates. Further cooling results in the transition from the liquid gel to the LC (nematic) gel. On heating, the two phase-transition endotherms are visible. Taking the maximums of the endothermic peaks as the transition temperatures, the phase diagram for E7/AG1 is obtained and shown in Figure 2. It is seen that the molecular aggregates of the gelator have little effect on the nematic–isotropic transition temperature of E7, i.e., the transition from the LC gel to liquid gel. However, the transition from liquid gel to liquid takes place at higher temperatures as the concentration of AG1 increases. These results were confirmed by observations on a polarizing microscope, where the transition from liquid to liquid gel is revealed by the appearance of birefringent aggregates while the transition from liquid gel to LC gel is accompanied by the appearance of the nematic texture of E7 filling in the space unoccupied by the aggregates. Moreover, visual tests were performed showing no flow of the mixtures once entering into the liquid gel state upon cooling. Infrared spectroscopy confirmed that the self-aggregation of AG1 is due to the formation of intermolecular hydrogen bonds. The characteristic bands for the two H-bonded C=O groups appear at 1632 (alkyl amide) and 1656 cm^{-1} (aromatic amide) in the liquid gel and LC gel states but absent in

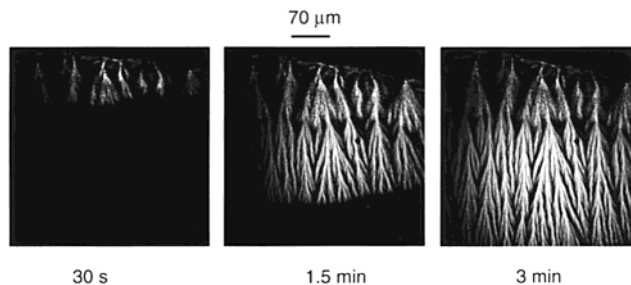


Figure 3. Polarizing optical micrographs taken at various times after cooling a film of E7/AG1 containing 0.5 mol % AG1 from the liquid phase to 100 °C. The film was cast on CaF_2 .

the liquid phase, shifted to 1665 and 1681 cm^{-1} for the C=O groups free of H-bonding. A higher liquid gel to liquid transition temperature reflects a greater stability of the H-bonded aggregates of AG1. The results in Figure 2 indicate that this stability increases as the concentration of the gelator increases. In addition to the thermal stability, measurements of the enthalpy of transition also suggest improved crystalline structures for the aggregates at higher concentrations of AG1, which was found to be 11.8, 18.9, 20.7, and 26.5 J/g for 0.2, 0.5, 1.0, and 1.7 mol % of AG1, respectively.

Surprisingly for AG1, the self-aggregation in E7 can lead to anisotropic liquid gel and LC gel at the macroscopic scale, without rubbed surfaces to induce the LC orientation or irradiation for optical alignment of azobenzene. Typically, when an E7/AG1 mixture was allowed to cool from the liquid phase to a temperature below but close to the sol–gel transition temperature, i.e., at a low degree of supersaturation, the aggregation process was found to start from the edge of the film, and fibrous aggregates grow in time in such a way that they lie predominantly normal to the edge of the film. This is illustrated by the set of optical micrographs shown in Figure 3, taken at various times after cooling a film, cast on a CaF_2 , of the mixture containing 0.5 mol % of AG1 to 100 °C. Within 3 min, the treelike aggregates of the gelator emerge from the edge and grow in the same direction to reach a length over 200 μm . Similar results were obtained for mixtures of various concentrations of AG1 and for films cast on both CaF_2 and glass slides. In all cases, once the aligned molecular aggregates were formed in the liquid gel state, further cooling to the LC gel did not affect the morphology of the H-bonded network. The striking feature of this self-assembly process is that the aligned fibrous aggregates can easily develop over a macroscopic area. For instance, in one particular experiment, a film of the mixture containing 1.0 mol % of AG1 was cast between two 8-mm-diameter circular glass slides; cooling the film from 140 to 115 °C for the gelation resulted in homogeneous fibrous aggregates all emerging, at the beginning, from the circular edge and converging, in the end, at the center of the film. Observations on SEM were made for this sample after extraction of E7. Figure 4a, at a low magnification, captures a region of the film displaying treelike aggregates perpendicular to the curved edge. Figure 4b, at a high magnification, shows the ribbonlike fibers (about 6 μm in width).

The macroscopically aligned fibrous aggregates may be the manifestation of an oriented H-bonded network of the gelator. Polarized infrared spectroscopy was used

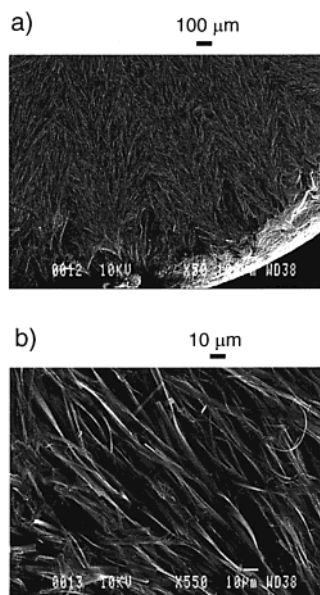


Figure 4. SEM pictures (top view) for a film of E7/AG1 containing 1.0 mol % AG1 at two different magnifications. The film was cast on glass slides and cooled from the liquid phase to 115 °C for aggregation of AG1; the pictures were taken at room temperature after extraction of E7.

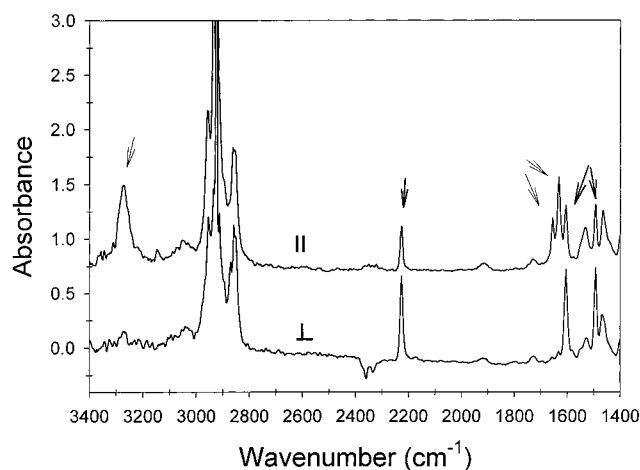


Figure 5. Polarized infrared spectra for a film of E7/AG1 containing 1.0 mol % AG1. Thin arrows in the figure indicate H-bonded N–H and C=O bands of the aggregates while thick arrows indicate the C≡N and phenyl bands of E7. The film was cast on CaF₂ and cooled from the liquid phase to 115 °C for aggregation of AG1. The two spectra were recorded at room temperature with the infrared beam polarized parallel and perpendicular to the fiber direction.

to analyze the molecular order in these materials. For all measurements, the sampling area was about 4 mm². Figure 5 shows the polarized infrared spectra for a film of 1.0 mol % of AG1, recorded at room temperature with the infrared beam polarized parallel and perpendicular to the fiber direction. In one hand, the two H-bonded C=O bands at 1632 and 1656 cm⁻¹ as well the H-bonded N–H band at 3274 cm⁻¹ of AG1, indicated by thin arrows, all exhibit strong parallel dichroism, indicating that the hydrogen bonds of the aggregates are oriented preferentially in the fiber direction. On the other hand, at room temperature the mixture is in the LC gel state, the C≡N band at 2227 cm⁻¹ and the phenyl bands at 1605 and 1493 cm⁻¹ assigned to E7, indicated by thick arrows, show perpendicular dichroism, indicating that

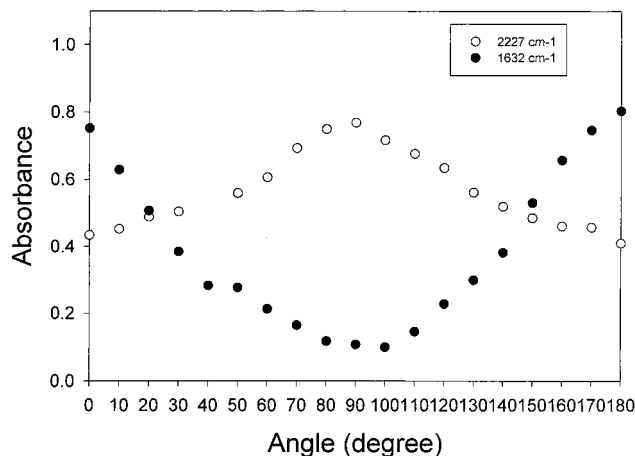


Figure 6. Absorbance of the infrared bands at 1632 (for H-bonded network) and 2227 cm⁻¹ (for E7) versus the angle between the fiber and infrared polarization direction for the same sample as in Figure 5.

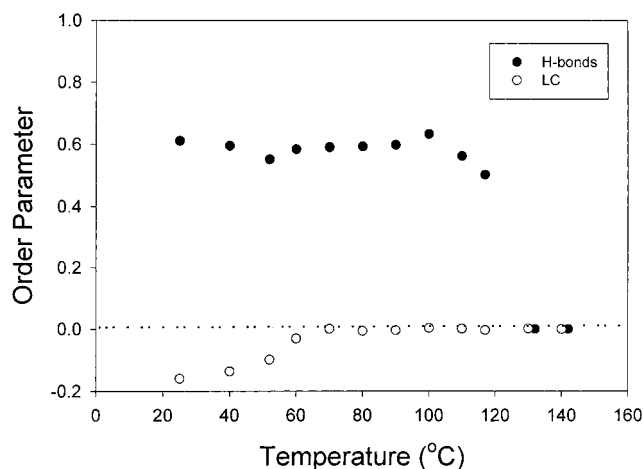


Figure 7. Order parameters of hydrogen bonds in the aggregates of AG1 and of E7 versus temperature for the same sample as in Figure 5.

the LC molecules in the LC gel are oriented preferentially normal to the fiber direction. To make sure that the apparent fiber axis points at the direction in which the H-bonds of the gelator line up uniaxially, infrared spectra were taken at various angles between the fiber and the infrared polarization directions. Plotted in Figure 6 are the absorbances of the bands at 1632 (for AG1) and 2227 cm⁻¹ (for E7) as a function of this angle, confirming the parallel orientation of the H-bonds in the molecular aggregates of AG1 and the perpendicular orientation of the LC molecules with respect to the fiber direction.

Furthermore, variable-temperature infrared measurements were performed on the self-assembled anisotropic gels. Order parameters S of the H-bonds in the aggregates and of E7 were determined from the 1632- and 2227-cm⁻¹ bands through $S = (A_{||}/A_{\perp} - 1)/(A_{||}/A_{\perp} + 2)$, where $A_{||}$ and A_{\perp} are the absorbances of the respective band with the infrared polarization parallel and perpendicular to the fiber direction. An example of the results is given in Figure 7, with the mixture containing 1.0 mol % of AG1. In the LC gel, the H-bonded network is highly anisotropic with S close to 0.6 for the H-bonds, while the long-range orientation of E7, having negative S , is perpendicular to the orientation direction of the

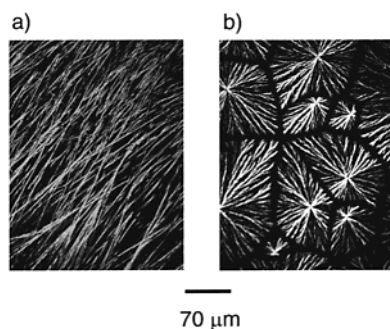


Figure 8. Polarizing optical micrographs for the mixture of E7/AG1 containing 0.5 mol % AG1. The film was cast on CaF_2 and cooled from the liquid phase (a) slowly to 105 °C for slow aggregation of AG1 and (b) rapidly to 90 °C for fast aggregation of AG1.

H-bonds. When the sample is heated to the liquid gel, the LC orientation is lost as E7 is in its isotropic phase, but the network (H-bonds) orientation remains intact. It is not until the gel–sol transition takes place at above 120 °C that the network anisotropy disappears. With the dissociation of the H-bonds in the liquid phase, the two C=O bands at 1632 and 1656 cm^{-1} are shifted to 1665 and 1681 cm^{-1} which show no infrared dichroism (the data points of $S = 0$ for AG1 in the liquid phase in Figure 7 are those from the new C=O bands). When the sample is cooled back from the liquid phase to the liquid gel state, the H-bonds orientation reappears while the E7 molecules remain unoriented; but once into the LC gel state on further cooling, the LC orientation comes back too, induced by the aligned aggregates. The recovered orientation of both the H-bonded network and E7 depends on the conditions for the aggregation process of AG1. If the cooling condition is the same as that initially used to prepare the anisotropic gel, the same orientation can be recovered.

The anisotropy of the H-bonded network and, as a result, the orientation of E7 are determined, to a large extent, by the morphology of the aggregates of the gelator which is sensitive to the kinetics of the sol–gel transition. The treelike fibrous aggregates shown in Figure 3 represent the morphology obtained under most conditions leading to aligned fibers (the average cooling rate from the liquid phase to the gelation temperature was about 8 °C/min). Figure 8 shows the other types of morphologies obtained under very slow and very fast aggregation. When the mixture containing 0.5 mol % of AG1 is cooled from 140 to 105 °C very slowly at 0.5 °C/min, the aggregation, still starting from the edge, is slow to develop, and the resulting fibers are thin, straight, and aligned. This morphology also induces the orientation of E7 in the LC gel state. In contrast, when the mixture is cooled rapidly (~ 8 °C/min) to 90 °C, which is deep below the sol–gel transition, i.e., at a large supersaturation, the aggregation is fast and starts from random nucleation centers throughout the sample. The aggregates grow by emanating from those centers, resulting in the flowerlike morphology. With this morphology no macroscopic orientation of the H-bonds is observed in the liquid gel, and no E7 orientation is induced in the LC gel state.

The orientation measurements were carried out at room temperature on anisotropic gels having different concentrations of the gelator. All samples were prepared

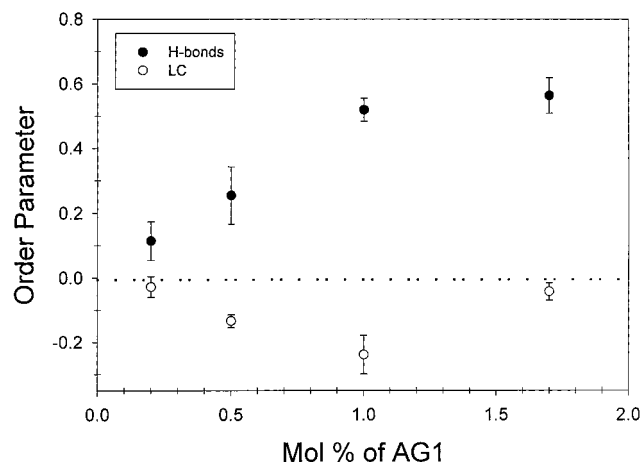


Figure 9. Order parameters of hydrogen bonds in the aggregates of AG1 and of E7 versus concentration of AG1 in the mixture. The films were cast on CaF_2 and cooled from the liquid phase to a temperature about 5 °C below the sol–gel transition temperature for aggregation of AG1.

by cooling from the liquid phase to a temperature close to the sol–gel transition (~ 5 °C below) for the development of the aggregates in the liquid gel, followed by further cooling to the LC gel. The results are shown in Figure 9, plotting the order parameters of both the network and E7 as a function of the concentration of AG1. The average values were calculated from measurements on different areas of the samples, and the error bars are the standard deviation. Two observations are worth being analyzed. First, as the gelator concentration increases until 1 mol %, a significant increase in the network as well as the LC orientation is observed. Higher LC orientation induced by more and better-aligned aggregates is what can be expected. However, at the highest concentration of AG1 (1.7 mol %), the network orientation remains high, but the induced LC orientation apparently drops. This result implies that the alignment of the aggregates is not the only important factor that determines the LC orientation. The extent of interaction between the two components may be another factor. At the highest gelator concentration studied, the degree of phase separation may become more severe and, consequently, the interfacial area with the LC molecules may actually decrease. SEM observations on the mixture containing 1.7 mol % of AG1 support this explanation, showing straight but much coarser fibrous ribbons of the aggregates than those arising from 1 mol % of AG1 (Figure 4b). The coarsened aggregates, although aligned, have less effective interaction with the E7 molecules. Second, Figure 9 shows that the orientation of the H-bonded network is lower at lower gelator concentrations. This may be related to the mechanism for the perpendicular fiber growth from the edge of the samples. When the concentration of the very first aggregates emerging from the edge of the film is high enough, while they grow in volume, any deviation or deflection from the trunks of the treelike fibers would be hindered by the steric interference from each other. The fibers would have the tendency to continue to grow in the same direction in order to ease the spatial constraints. While with fewer aggregates starting from the edge, deflection into other directions would be easier because of more space available between the fibrous aggregates, resulting in more disorder.

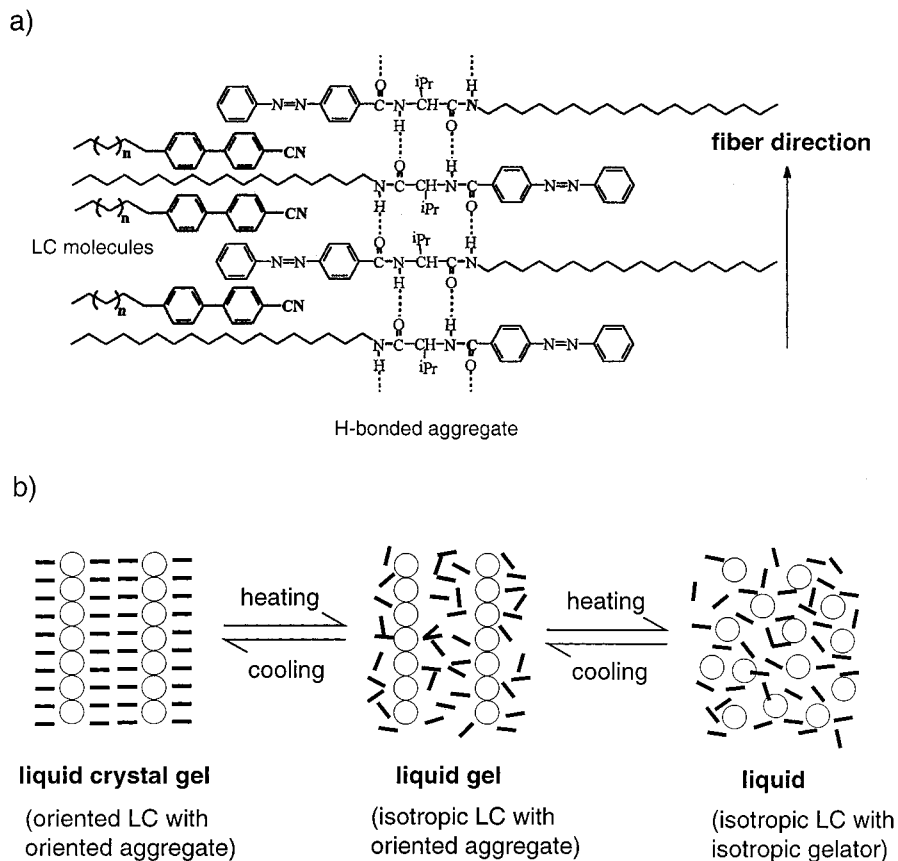


Figure 10. Sketch illustrating (a) the one-dimensional array of the intermolecular hydrogen bonding of the gelator, forming the unit fiber of the aggregates, as well as the perpendicular anchoring of the E7 molecules at the interface with the fibers, and (b) the anisotropy developed in the self-assembly process. The rods and circles in (b) represent the E7 and gelator molecules, respectively.

On the basis of the above infrared results, Figure 10 schematically recapitulates the way the oriented molecular aggregates of AG1 are self-assembled through the formation of H-bonds. The unit fiber should be formed from the succession of the intermolecular H-bonds formed by the two amide groups. The depicted antiparallel stacking of the AG1 molecules should be favored since four H-bonds are involved instead of two for the parallel stacking. The fiberlike aggregates are built up from those one-dimensional molecular arrays by condensation. Because of the low concentration of AG1 and superimposition of the bands, infrared spectra cannot be used to assess the order of the long alkyl chains and the azobenzene moieties in the aggregates. Nevertheless, for azobenzene groups it is easy to picture that they should be mostly normal to the fiber direction. This may account for the perpendicular anchoring of the E7 molecules at the interface with the H-bonded network because of the affinity and interaction between the azobenzene and cyanobiphenyl molecules. The E7 molecules directly in contact with the interface may tend to align molecules more distant from the interface in the same direction, which results in the observed perpendicular LC orientation. The various levels of anisotropy during this self-assembly process are also summarized in the sketch. In the liquid state, both components are in the isotropic phase. In the liquid gel state, an aligned H-bonded network emerges, which gels the isotropic LC. Finally, in the LC gel state, the aligned network induces a long-range LC orientation. But to fully understand the mechanism of aggregation and LC

orientation induction as well as the structure of the aggregates, the use of techniques such as X-ray diffraction will be needed.

Two questions should be asked. Why does the aggregation start from the edge? And why do the fibrous aggregates grow perpendicular to the edge? To answer the first question, a number of experiments were performed. First, films were allowed to cool under nitrogen atmosphere through the sol-gel phase transition, and the same phenomenon was observed. This result suggests that the interaction, if there is any, between oxygen molecules in air and the gelator is not what causes the aggregation from the edge. Second, since temperature changes trigger the driving force for the sol-gel phase transition, another possible explanation is a temperature gradient established during the cooling of the samples inside the hot stage. Especially for films sandwiched between two windows, it is reasonable to think that the edge of the film may need a shorter time to reach the temperature of air than the central part of the film separated from air by the windows. However, the results of two experiments seem to rule out this scenario. In one, films cast between two windows were cooled very slowly at a rate of 0.5 °C/min; at such a cooling rate thermal equilibrium should have enough time to reach for the whole film. In the other, films were cast on one single window, with the film surfaces in the open air during the experiment. In both cases, the aggregation was found to start from the edge. A third possible explanation is the existence of a concentration gradient of AG1 in the mixture with E7.

If the concentration of the gelator is slightly higher at the edge of the films, the aggregation should start there because of a higher sol–gel transition temperature. Another speculation is that the surface tension on the edge is different from other part of the film. At this point of time, we cannot confirm these hypotheses.

For the second question as to know why the fibers grow perpendicular to the edge, a qualitative analysis can be made. As already mentioned and sketched in Figure 10, the one-dimensional arrays of H-bonded AG1 molecules are the building blocks for the observed fiberlike aggregates. The first arrays formed on the edge of the film, which serve as the nucleation centers for further growth of the aggregates, would prefer to lie normal to the interface between the film and air, since parallel alignment would mean that a number of the alkyl chains of the arrays must cross the boundary, which, energetically, should not be favored. Once the first fibers are established perpendicular to the edge, continuous growth is likely in the same direction by adding and lining up the H-bonds.

Underway in our laboratory are studies that apply irradiation to the azobenzene-containing gelator and

investigate the effects of irradiation on the properties of the LC anisotropic gels. Results will be reported later.

Conclusion

The new azobenzene-containing gelator AG1 is able to gel nematic LCs such as E7. For thin films cast on CaF₂ windows or glass slides whose surfaces are not rubbed, if the aggregation of AG1 through the formation of intermolecular hydrogen bonds is allowed to proceed at temperatures close to the sol–gel phase transition temperature, fibrous aggregates start to form at the edge of the films and grow mainly perpendicular to the edge. This self-assembly process leads to the formation of a macroscopically oriented H-bonded network in the liquid gel, which, in turn, can induce a long-range LC orientation in the LC gel state.

Acknowledgment. We thank M. Pierre Magny for assisting the electron microscopy observations. Financial support from the Natural Sciences and Engineering Research Council of Canada and the Fonds pour la Formation de Chercheurs et l'Aide à la Recherche of Québec is acknowledged.

CM000571Q